Title	Snow as a Locking Material : High Pressure Properties of Snow
Author(s)	Hanagud, S.
Citation	Physics of Snow and Ice : proceedings, 1(2), 807-826
Issue Date	1967
Doc URL	http://hdl.handle.net/2115/20344
Type	bulletin (article)
Note	International Conference on Low Temperature Science. I. Conference on Physics of Snow and Ice, II. Conference on Cryobiology. (August, 14-19, 1966, Sapporo, Japan)
File Information	2_p807-826.pdf

Snow as a Locking Material
— High Pressure Properties of Snow —

S. HANAGUD

Stanford Research Institute, Menlo Park, California, U.S. A.

Abstract

This paper discusses the properties of snow at high pressures. In particular the possibility of considering snow as a multistage inhomogeneous locking material under high pressures and impact loading has been investigated. Some uniaxial wave propagation problems under these assumptions have been considered. Finite displacements and inhomogeneous distribution of initial density have been considered. The behavior of snow under these assumptions and subjected to impact loading has been discussed. The resulting stresses and velocities have been calculated by numerical methods.

Also the possibility of using impact tests and shock propagation to determine the mechanical properties of snow has been discussed.

Locking material is an ideal material or a mathematical approximation of certain real materials. These materials are characterized by the particular property that they offer on increasing to deformation as the deformation increases. They may also be called as foamed or compactible materials.

I. Introduction

Extensive investigations have been conducted in the past to determine the mechanical properties of snow. Most of the work concerns the determination of the properties, such as the modulus of elasticity, Poisson's ratio, shear strength, tensile strength, creep properties, acoustic properties, etc. Some of the application of such investigations have been the prediction of settlement of structures supported by dry ice caps (Costes, 1963; Anderson and Benson, 1963), to develop techniques of producing high strength snow by compaction (Wuori, 1963).

In these studies the magnitude of pressure has been very small; for example, the maximum compressive stress in Mellor's (Mellor, 1962) work was only about 44 atmospheres. It is well known, however, that the properties of materials can be studied at very high pressures and under high rates of loading.

Such a study will be very useful in predicting the dynamic behavior of snow under the application of very high pressures. These investigations might provide answers to many practical problems, such as the effect of a sudden application of pressure on protective structures, shock wave propagation, and attenuation of peak pressures in snow.

The purpose of this paper is then to discuss the basic problems involved in the study of the properties of snow and the dynamic response of snow at high pressures.

II. Constitutive Relations

The properties of snow as required in this study can be specified by a set of con-

stitutive relations. To be very precise, these relationships must include the thermodynamic effects. A mathematical formulation of such relationships would need some mechanical or thermodynamic variables. These variables can be selected from:

1. The stress tensor σ
2. The strain tensor ε
3. The temperature Θ
4. The specific entropy η
5. The internal energy e

Specification of certain relationships between these variables, must be based on thermodynamic principles and experimental evidence. It can be assumed:

1. That there exists a relationship among the stress, strain, and specific entropy. Such a relationship, may include stress rates, strain rates, or the effects of memory (Noll and Truesdell, 1964).

2. That furthermore, the temperature can be assumed to be a function of strain and specific entropy. These two relationships are written in the form of equations as

$$\sigma = \sigma\,(\varepsilon, \eta), \tag{1}$$

$$\Theta = \Theta\,(\varepsilon, \eta). \tag{2}$$

Sometimes, the variable temperature Θ is replaced by the variable internal energy e. A relationship among the internal energy, the strain, and the entropy is assumed to exist. This relationship is usually called the caloric equation of state.

$$e = e\,(\varepsilon, \eta). \tag{3}$$

Very often equations such as

$$\sigma = \sigma\,(e, \varepsilon), \tag{4}$$

which relate the stress tensor, strain tensor and internal energy are very useful in the study of shock propagation. Such equations can be called incomplete equations of state or mechanical equations of state.

In addition to the aforementioned relationships the following are necessary:

3. A relationship among the heat flux, temperature gradient, strain, and specific entropy to complete the set of constitutive relations.

4. Certain requirements through which the constitutive relations satisfy the usual principles of invariance (Noll and Truedell, 1964).

III. Structure of Snow

In the absence of experimental results it is very difficult to write the explicit forms of eqs. (1)–(4). However constitutive relationships can be built on the available knowledge of the physical properties of snow. These relationships can be improved later to suit the realistic behavior of snow.

According to the observed physical properties, initially the polar snow has the consistency of table salt (Mellor, 1962) with a grain size of approximately 0.1 to 1 mm. However, after deposition the intergranular bonds begin to form with sublimation. Such growth of grain and the bond development changes snow from the consistency of the

table salt to that of styrofoam. Snow in this state can actually be sawed into blocks like styrofoam. Snow is then a porous solid.

When new layers of snow are deposited, the older layers of snow are buried. The buried snow is then compressed, and this compression results in a porous solid whose porosity varies with the depth. The density at the surface is about 0.35 to 0.4 g/cm³ but about 30 m below the density can vary between 0.6 and 0.9 g/cm³.

Yosida (1962) has made a valuable contribution to our knowledge of the physical properties of snow. He has been able to observe the microstructure of a thin slice and has shown that the structure of snow is made of thin needles of ice linked together. This shows that snow, is in fact, a porous solid of varying porosity with a micro-structure, being made of thin needles of ice linked together. Graphite foam, in fact, has a similar microstructure to snow.

IV. Behavior of Snow under Hydrostatic Pressure

The mechanical behaviour under the application of uniform hydrostatic pressure can now be discussed. The application of the pressure reduces the volume. As the pressure is increased, the needle-like structure of the snow collapses, and the porosity decreases appreciably under a moderate increase of pressure. During this process of deformation, a small amount of pressure will produce an appreciable amount of decrease in the volume. However, as the volume decreases and the pore spaces collapse, the snow becomes denser, and it becomes harder and harder to compress and further reduce the volume.

At high values of pressure the snow attains the density of the ice, or a value very near to that. Additional pressure will cause the material to deform like ice. In this process, the temperature variation has not been considered. It has been assumed that the temperature remains the same and that the rate of loading is slow enough for the process to be considered static loading.

This behavior has been illustrated by lines AB of Figs. 1–3. The initial density of snow is 0.4 g/cc in Fig. 1. If the initial density were different, the curve on the $p-v$
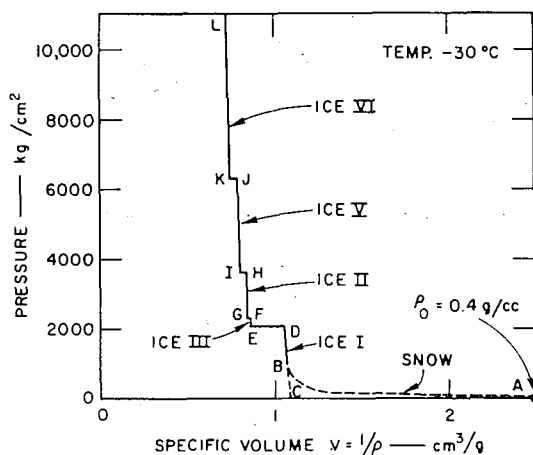

Fig. 1.

diagram would be different, as shown in Fig. 2 for an initial density of 0.5 g/cc. However, as the compressive stress increases the density of ice is attained in both cases. The figure has been platted as a $p-v$ diagram with pressure in kg/cm²* and the specific volume v in cm³/g.

After the material has attained the density of ice, the material can be expected to deform like ice. This behavior depends very much on the temperature (Bridgeman, 1912) and exhibits different types of phase transition (Bridgeman, 1912, 1914, 1937, 1941).

In Fig. 1, it is assumed that the temperature is −30°C and that it remains the same as the snow is compressed. As was explained above, the material will attain the density of ice or a value very near to that at a pressure P_1. Later snow at this temperature and pressure can be considered to be in the form of ice I (Bridgeman, 1911). The curve BD indicating the deformation of ice I is from Bridgeman's data. However, the slopes of the curves are based on the data along the equilibrium curves. When the value of the hydrostatic pressure attains a value of 2 150 kg/cm², a phase change transforms the material from the ice I to ice III, and a sudden reduction in specific volume of 0.192 cm³/g takes place. Such phase changes occur as changes of volume under constant pressure (Bridgeman, 1912) when the rate of application of pressure is slow enough for the process of loading to be considered static. This behavior is shown by the straight line DE of Fig. 1.

Further increases in pressure will result in a phase change from ice III to ice II at a pressure of about 2 300 to 2 400 kg/cm². This phase change results in a sudden reduction of the specific volume of 0.017 cm³/g at constant pressure. This is shown by the straight line FG of Fig. 1.

As the pressure is increased beyond the value of 2 400 kg/cm² and if the temperature still remains at −30°C, a phase change will take place at a pressure of about 3 700 kg/cm², changing ice II to ice V. This phase change causes a reduction of the volume by an amount of 0.04 cm³/g. This is shown by the line HI of Fig. 1.

Another phase change will occur at a pressure of 6 300 kg/cm², changing the ice V to ice VI and reducing the specific volume by about 0.038 cm³/g. The phase change from ice VI to ice VII at a pressure of about 22 300 kg/cm² has not been shown in the figure. This phase change will cause a reduction of the specific volume by about 0.054 cm³/g.

Thus, the compression of snow at −30°C from 0 to 10 000 kg/cm² follows the path AB, BD, DE, EF, FG, GH, HI, IJ, JK and KL of Fig. 1.

V. Properties at Different Temperatures

Figure 2 illustrates the compression of snow at −22°C. As in the preceding case, the snow compresses to ice I along a path, such as AB. Then the material follows the curve BD as Ice I until the occurrence of the phase change from ice I to ice III at a pressure of about 2 100 kg/cm². However, in this case, the phase change will *not* occur from ice III to ice II. The material will continue to behave like ice III up to 3 500 kg/cm². When a phase change occurs from ice III to V, reducing the specific
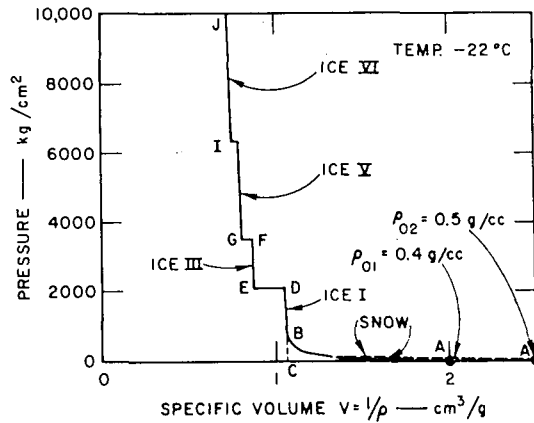
---

* Kilogram (weight)/cm² = 0.96784 atmosphere = 14.223 lb/in².

Fig. 2.

volume by about 0.054 cm³/g. Later, the behavior is very similar to that illustrated in Fig. 1 for a temperature of $-30°C$.

A comparison of Figs. 1 and 2 shows that the behavior is slightly different because of the phase change from III to II. Of course, the reduction of the specific volume during this change is very small compared to that during other phase changes. The $P-V$ curves at these temperatures $(-22$ and $-30°C)$ do not differ much. However, the $P-V$ curve for a temperature of 0°C is quite different from the $P-V$ curves in Fig. 1 or 2. The initial compression of snow to ice is very similar to that of Figs. 1 and 2. However the ice I immediately changes to water. Later the material compresses like water until a pressure of about 6 300 kg/cm² is reached. At this pressure water changes to ice VI. Later the material behaves like ice VI. These processes are illustrated by the lines AB, BC, CD, DE and EF in Fig. 3. The line DE illustrates the phase change from water to ice VI. The reduction in specific volume is 0.09 cm³/g.

Figures 1–3 illustrate that the thermodynamic effects are important if the temperature change caused by the shock wave is more than a few degrees centigrade.
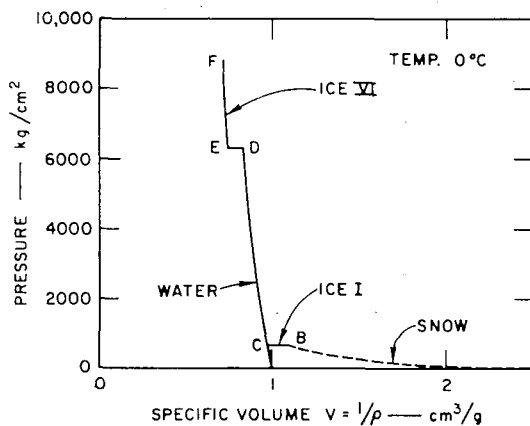

Fig. 3.

VI. Shock Waves and the Constitutive Relations

If a knowledge of the constitutive relations is available, the shock velocity and the particle velocity behind the shock wave can be predicted. However, if the shock velocity, particle velocity, and other changes across the shock wave can be measured, constitutive relations can be obtained. Such techniques have been used by measuring steady state shock in certain materials (Rice *et al.*, 1958; Duvall, 1962 a, 1962 b; Doran and Linde, 1966). However in cases such as snow some more knowledge regarding the general form constitutive relationship might be necessary before such measurements can be used to determine the constitutive equations precisely. This knowledge, however, requires experimentation. By a suitable cooperative experimental and theoretical study and the use of the shock wave techniques, the constitutive relations can be determined.

VII. Snow as a Locking Material

In the absence of any such experimental results the following approach has been selected to predict the dynamic behavior of snow at high pressures.

1. It will be assumed that the temperature changes due to the shock wave are so small that the thermodynamic effects can be neglected. This means that for a given initial temperature a definite relationship between the pressure and the specific volume is given. In practice, there will be a temperature change across the shock wave. This effect, if appreciable, will be observable in experiments, as a deviation from the theory. The theory in turn could later be improved.

2. The static behavior discussed in the preceding sections will be assumed to be valid during dynamic changes. This is also not true in general. However the static behavior usually provides steady state stress profiles. These results can be used to improve the theory (Duvall, 1963; Hanagud, 1966) and build in dynamic transient response.

3. Furthermore the curves will be approximated by straight lines, as shown in Fig. 4. Figure 4 shows the diagram with the straight lines BC, DE and FG parallel to the
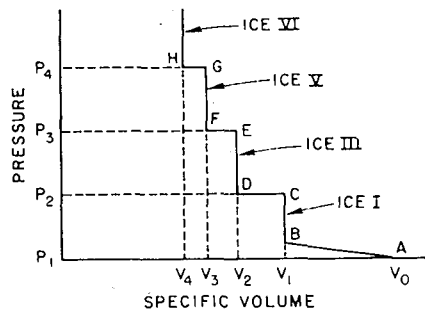

Fig. 4.

axis representing pressure. This means that snow on application of pressure collapses along AB to become ice I. Later the specific volume remains at the value V_1 corresponding to ice I until the pressure reaches a value of P_2 and the ice I suddenly changes to ice III. The specific volume now corresponds to the value V_2 and does not change

until the hydrostatic pressure has been increased to the value of P_3, when the ice III will change to ice V and the new specific volume will be V_3. Similar change from ice V to ice VI takes place at a pressure P_4.

Such an approximation would be valid for a temperature range between -22 to $-30°C$. The ideal material resulting from such an approximation and shown in Fig. 4 can be called a multistage locking material. The meaning of this term will be explained in the next section.

VIII. Locking Material

Locking or compactible materials (Prager, 1956 a, 1956 b; Grigorian, 1956; Flugge and Hanagud, 1963) are idealizations of real material. Such an idealization simplifies the analysis while keeping some essential physical characteristics of the real material. A single stage locking material can be explained by considering the following example.

Consider sponge or polyurethane foam and apply hydrostatic compression to such a material. Initially a small amount of pressure will produce an appreciable amount of deformation or reduction in volume. As the pressure is increased the density of the material continues to increase with the increase in density, the material offers an increasing amount of resistance to deformation, ultimately the sponge or polyurethane foam will attain a state in which very large amounts of pressure will produce very little reduction in volume when compared with similar reductions in volume at the initial states. Such a relationship can be qualitatively shown in the form of Fig. 5. The curve OEC illustrates the possible experimental curve. Such a curve can be approximated by
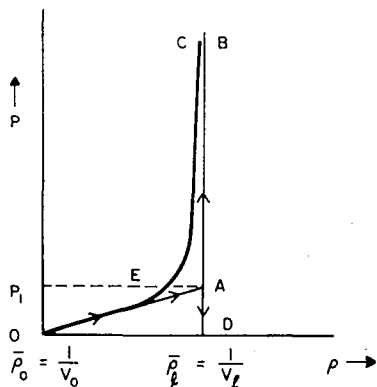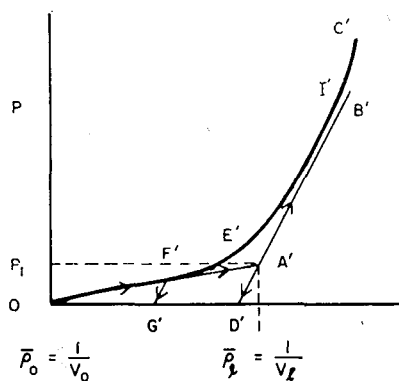

Fig. 5.

Fig. 6.

two straight lines OA and AB. This means that the sponge can be compressed along OA until the specific volume attains a value of V_l. Later the specific volume remains at the value of V_l while pressure can increase indefinitely. Such a material is called ideal locking material. Often the small decrease in specific volume after locking cannot be neglected. Then the curves can be approximated by two straight lines, such as OA' and AB' (Fig. 6). Such a material is called non-ideal locking material. These are single stage locking materials whereas snow (Fig. 4) is a multistage locking material, because the material locks at specific volumes (V_1, V_2, V_3, V_4) only during a certain pressure

range, such as between P_1-P_2, P_2-P_3, P_3-P_4 etc. At the values of pressure P_2, P_3 and P_4 the material suddenly collapses into a different locked state. For example, when the pressure attains a value of P_1 the snow is said to be locked in the state of ice I. Similarly the snow will be locked in the state of ice III when the pressure P_2 is attained.

In this paper only two stage locking will be considered. This means the pressure will be limited to about 4 000 atmospheres at a temperature between -22 to $-30°C$. At higher pressures the consideration of temperature changes across the shock wave might be important.

Furthermore the initial density will be assumed to vary with the position in space. This will take care of the varying density with depth in snow. Thus the idealization of snow considered in this paper is an inhomogeneous, multistage ideal locking material. Further improvements can later be done to improve the theory.

IX. Case of Uniaxial Strain and Finite Deformations

Most of the experiments (Rice et al., 1958; Duvall, 1962 a, 1962 b; Doran and Linde, 1966) in the study of shock waves in solids have been conducted under conditions which simulate uniaxial strain. Let x be the axis of a cartesian coordinate system x, y, z along which the material is permitted to strain. Then the conditions of uniaxial strain are

$$u = u(x, t),\qquad(5)$$
$$v = w = 0,$$

where u, v and w are velocities in x, y and z directions, and x is the Eulerean coordinate. The only nonzero component of the rate of strain is

$$\dot{\varepsilon}_x = \frac{\partial u}{\partial x}.\qquad(6)$$

Other strain rates are equal to zero.

$$\dot{\varepsilon}_y = \dot{\varepsilon}_z = \dot{\gamma}_{xy} = \dot{\gamma}_{yz} = \dot{\gamma}_{zx} = 0.\qquad(7)$$

The nonvanishing components of stress tensor are σ_x, σ_y and σ_z. They can be written as

$$\sigma_x = -P + D_x,\qquad(8)$$
$$\sigma_y = \sigma_z = -P + \tfrac{1}{2}D_x,\qquad(9)$$

where

$$-P = (\sigma_x + 2\sigma_y)/3,\qquad(10)$$
$$D_x = 2(\sigma_x - \sigma_y)/3,\qquad(11)$$

$\sigma_y = \sigma_z$ under conditions of uniaxial strain because the velocities in Y and Z directions are zero, and the direction of Y or Z is arbitrary with respect to the X direction. The deformations can be quite large because of the possible large reductions in specific volume, as shown in Figs. 1 to 3. Therefore instead of the usual assumption of infinitesimal displacements finite deformations will be considered.

Furthermore, the initial density ρ_0 will be assumed to be a function of x; i.e.,

$$\rho(t = 0, x) = \rho_0(x).\qquad(12)$$

This will represent a one-dimensional sample of snow with x-axis in the direction of

the depth.

X. Stress-Strain Relationship

The relationship between $P = -(\sigma_x + 2\sigma_y)/3$ and the density variation will be according to the assumption of multistage locking material (Fig.4).* In the first case to be considered the material will be assumed to have no shear resistance, $i.e.$,

$$\sigma_x - \sigma_y = 0 . \tag{13}$$

Later an elastic-plastic behavior will be assumed. More realistic behavior would need a complicated relationship between $(\sigma_x - \sigma_y)$ and the rate of shear strain.

XI. Problem of Finite Amplitude Wave Propagation

In the one-dimensional system under conditions of uniaxial strain, a stress $\sigma_x = -\bar{P}(t)$ is assumed to be applied at the time $t=0$ at the left boundary $x=a(t)$. Initially for $t=0$ the material is assumed to be at rest, stress free, and $a(0)=a_0$.

As a result of the applied pressure certain regions of the material will be disturbed. The disturbed region may consist of one or many discontinuity surfaces or shock waves.

XII. Case of $P < P_2$

If the stress $(-\sigma_x)$ applied at $x=a(t)$ is less than P_2, there the region will consist of only one shock wave. Let the position of the shock wave front be denoted by $x=k(t)$. Then in the region $a(t)<x<k(t)$, the following equation of motion can be written.

(a) *Newton's law*

$$\rho\left(u\frac{\partial u}{\partial x}+\frac{\partial u}{\partial t}\right) = \frac{\partial \sigma_x}{\partial x} . \tag{14}$$

(b) *Conservation of mass*

$$-\frac{1}{\rho}\left(u\frac{\partial \rho}{\partial x}+\frac{\partial \rho}{\partial t}\right) = \frac{\partial u}{\partial x} . \tag{15}$$

For any pressure $P > P_1$ (P_1 has been assumed to be equal to zero). The material is in the locked state, $i.e.$, in the disturbed region $a(t)<x<k(t)$

$$\rho = \rho_{l1} , \tag{16}$$

where ρ_{l1} is a constant and is equal to the first stage locking density. Then eq. (15) can be integrated to yield

$$u = f(t) . \tag{17}$$

Then eq. (14) becomes

$$\frac{\partial \sigma_x}{\partial x} = \rho \dot{f}(t) , \tag{18}$$

where the dot represents differentiation with respect to time. Then

$$\sigma_x = \rho_{l1} x \dot{f}(t) + g(t) . \tag{19}$$

---

* P_1 has been assumed to be zero. On any increase of pressure the material is assumed to collapse from any initial density ρ_0 to the locking density ρ_l.

$g(t)$ is an arbitrary function of time.

The functions $f(t)$, $g(t)$, $k(t)$ and $a(t)$ must be determined by appropriate boundary conditions.

At the left boundary $x=a(t)$ certain stress $\sigma_x=-\bar{P}(t)$ is prescribed.

Then
$$g(t) = -\bar{P}(t)-\rho_{l1}a(t)\dot{f}(t),\qquad(20)$$

and
$$\sigma_x = \rho_{l1}(x-a)\dot{f}(t)-\bar{P}(t).\qquad(21)$$

At $x=k(t)$ the appropriate jump conditions should be satisfied. The two jump conditions are

(a) *Conservation of mass*
$$x = k(t),\qquad \rho_{l1}(\dot{k}-u) = \rho_0(k)(\dot{k}).\qquad(22)$$

(b) *Conservation of momentum*
$$x = k(t),\qquad \rho_{l1}(\dot{k}-u)u = -\sigma_x.\qquad(23)$$

From eq. (22)

$$x = k(t),\qquad u = \dot{k}\left[1-\frac{1}{\rho_{l1}}\rho_0(k)\right]\qquad(24)$$

Hence from eq. (17)

$$f(t) = \dot{k}\left[1-\frac{1}{\rho_{l1}}\rho_0(k)\right].\qquad(25)$$

A simple variation of initial density will be considered.

$$\rho_0(x) = \bar{\rho}_0\left(1+\alpha\frac{x}{L}\right)\qquad \text{for}\quad x\leq L,\qquad(26)$$

$$= \bar{\rho}_0(1+\alpha)\qquad \text{for}\quad x\geq L.\qquad(27)$$

When $\alpha=0$ the solution for constant initial density can be obtained. The discussion unless specifically mentioned will be restricted for $x\leq L$.

Equation (25) then becomes

$$f(t) = \dot{k}\left[1-\frac{\bar{\rho}_0}{\rho_{l1}}\left(1+\alpha\frac{k}{L}\right)\right]\qquad(28)$$

This equation can also be written as

$$f(t) = \beta\dot{k}-\eta k\dot{k},\qquad(29)$$

where

$$\beta = 1-\frac{\bar{\rho}_0}{\rho_{l1}},\qquad \eta = \frac{\alpha}{L}\frac{\bar{\rho}_0}{\rho_{l1}}.\qquad(30)$$

Then the expression for σ_x (eq. 21) becomes

$$\sigma_x = \rho_{l1}(x-a)(\beta\ddot{k}-\eta\dot{k}^2-\eta k\ddot{k})-\bar{P}(t).\qquad(31)$$

Equations (23) and (31) then result in the following equation:

$$-\rho_{l1}(k-a)(\beta\ddot{k}-\eta k\ddot{k}-\eta\dot{k}^2)+\bar{P}(t) = \rho_{l1}(\dot{k}-\beta\dot{k}+\eta k\dot{k})(\beta\dot{k}-\eta k\dot{k}).\qquad(32)$$

Equation (32) is a differential equation in $k(t)$ and $a(t)$. $a(t)$ can be eliminated from this equation by considering the conservation of mass of the region $x<k(t)$.

The displacement at the wave front $x = k(t)$ is zero because of the continuity of displacement at the wave front. Therefore the mass occupied initially ($t = 0$) in the region $0 < x < k(t)$ is now occupying the region $a(t) < x < k(t)$. Therefore,

$$\int_0^{k(t)} \rho_0(x)\,\mathrm{d}x = \rho_{l1}(k - a) . \tag{33}$$

For $\rho_0(x)$ as assumed in eqs. (26) and (27)

$$\bar{\rho}_0 \left(k + \frac{\alpha k^2}{2L} \right) = \rho_{l1}(k - a) . \tag{34}$$

Equation (32) now can be written as

$$\left(k + \frac{\alpha k^2}{2L} \right)\left(1 - \frac{\eta}{\beta} k \right)\ddot{k} - \left(k + \frac{\alpha k^2}{2L} \right)\frac{\eta}{\beta}\dot{k}^2 + \dot{k}^2\left(1 + \eta\frac{\rho_{l1}}{\bar{\rho}_0} k \right)\left(1 - \frac{\eta}{\beta} k \right) = \frac{\bar{P}(t)}{\bar{\rho}_0\beta} . \tag{35}$$

If eq. (35) can be solved for $k(t)$ subject to appropriate initial conditions, $\sigma x, u$ and a can be obtained from eqs. (31), (24) and (34). The initial conditions are

$$t = 0 , \qquad k = 0 , \qquad \dot{k} = \left(\frac{\bar{P}(0)}{\bar{\rho}_0\beta} \right)^{1/2} . \tag{36}$$

Solution of eq. (35). Two cases will be studied. The first case will consider a constant initial density $\bar{\rho}_0$. The second case will consider the variation of density as specified in the preceding section. The stress boundary condition will be

$$(\sigma_x)_{x=a(t)} = -\bar{P} \quad \text{for} \quad 0 < t < \bar{t}; \quad \bar{P} = 0 \quad \text{for} \quad t > \bar{t} . \tag{37}$$

Case of constant density. When the initial density is constant $\alpha = 0$ and $\eta = 0$. Then eq. (36) becomes

$$k\ddot{k} + \dot{k}^2 = \frac{\bar{P}(t)}{\bar{\rho}_0\beta} . \tag{38}$$

For $0 < t < \bar{t}$ the solution is simply

$$\dot{k} = \left(\frac{\bar{P}}{\bar{\rho}_0\beta} \right)^{1/2} , \tag{39}$$

or

$$k = \left(\frac{\bar{P}}{\bar{\rho}_0\beta} \right)^{1/2} t . \tag{40}$$

The shock wave propagates at a constant velocity. For $t > \bar{t}$, eq. (38) becomes

$$k\ddot{k} + \dot{k}^2 = 0 . \tag{41}$$

This equation can be integrated once with respect to t to yield

$$\log_e \dot{k} = -\log_e k + \log_e A , \tag{42}$$

where A is a constant. This equation can be written as

$$k\dot{k} = A , \tag{43}$$

or

$$k\,\mathrm{d}k = A\,\mathrm{d}t . \tag{44}$$

Hence

$$k = (2At + B)^{1/2} , \tag{45}$$

and

$$\dot{k} = \frac{A}{(2\bar{A}t+B)^{1/2}} . \tag{46}$$

The initial conditions to determine A and B are

$$t = \bar{t} , \quad \dot{k} = \left(\frac{\bar{P}}{\bar{\rho}_0\beta}\right)^{1/2} , \quad k = \left(\frac{\bar{P}}{\bar{\rho}_0\beta}\right)^{1/2} \bar{t} . \tag{47}$$

Then,

$$A = \left(\frac{P}{\bar{\rho}_0\beta}\right)\bar{t} , \quad B = -\frac{\bar{P}}{\bar{\rho}_0\beta} \bar{t}^2 .$$

Then

$$k = \sqrt{\frac{\bar{P}}{\bar{\rho}_0\beta}} (2t\bar{t}-\bar{t}^2)^{1/2} , \tag{48}$$

$$\dot{k} = \sqrt{\frac{\bar{P}}{\bar{\rho}_0\beta}} \{\bar{t}/(2t\bar{t}-\bar{t}^2)^{1/2}\} . \tag{49}$$

Equations (48) and (49) show that the wave front $k \to \infty$ as $t \to \infty$ while the wave velocity $\dot{k}$ and hence the stress tend to zero as $t \to \infty$. These are the results that can be expected after unloading.

If P_1 were not equal to zero an elastic wave will be present in the material.

Figure 7 shows the position of the wave front as a function of time. Variation $(-\sigma_x/\bar{P})$ at the wave-front with $t/\bar{t}$ is illustrated in Fig. 8.

Case of varying initial density. For the case of varying initial density a simple solution is not possible. Equation (36) has been integrated using a digital computer. The equation is nondimensionalized by the use of the following variables
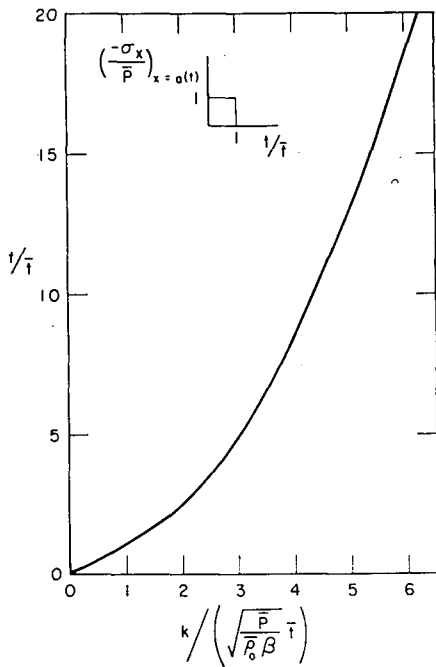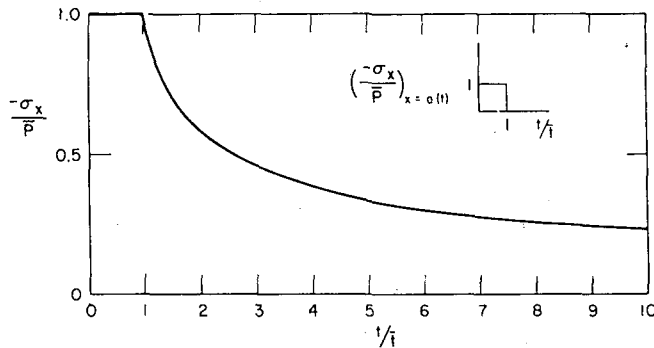
Fig. 7.

Fig. 8.

$$q = \frac{k}{L} \; . \tag{50}$$

$$T = \sqrt{\frac{\overline{P}(0)}{\overline{\rho}_0 \beta}} \; \frac{1}{L} \, t \; . \tag{51}$$

Then, eq. (36) becomes

$$\left(q + \frac{\alpha q^2}{2} \right) \left(1 - \frac{\xi}{\beta} q \right) \cdot \frac{\mathrm{d}q^2}{\mathrm{d}T^2} - \left(q + \frac{\alpha q^2}{2} \right) \frac{\xi}{\beta} \left(\frac{\mathrm{d}q}{\mathrm{d}T} \right)^2$$
$$+ \left(1 + \frac{\xi \rho_{l1}}{\overline{\rho}_0} q \right) \left(1 - \frac{\xi}{\beta} q \right) \left(\frac{\mathrm{d}q}{\mathrm{d}T} \right)^2 = \frac{\overline{P}(t)}{\overline{P}(0)} \; . \tag{52}$$

In eq. (52)

$$\xi = \alpha \frac{\overline{\rho}_0}{\rho_{l1}} = \eta L \; . \tag{53}$$

The results are shown in the form of Figs. 9 and 10. Figure 9 shows the position
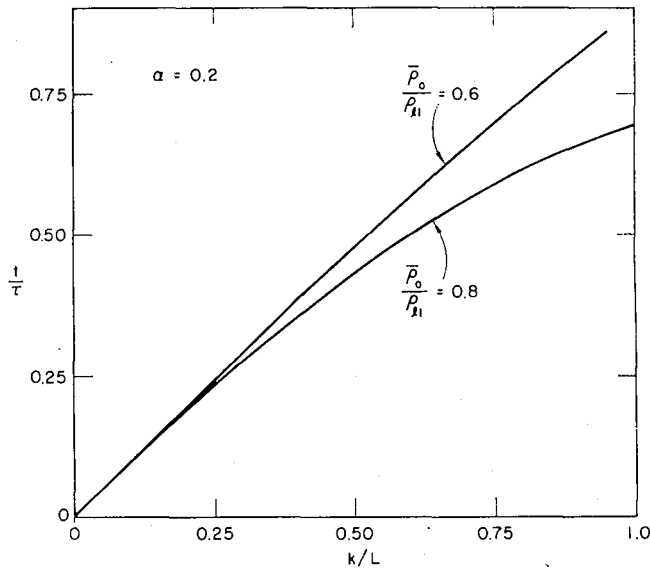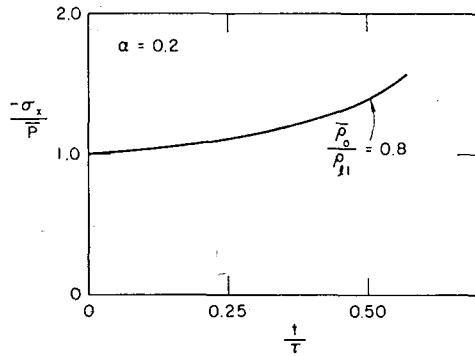

Fig. 9.

Fig. 10.

of the wave front as a function of time for two different cases* of varying initial density. The wave velocity increases as x increases because the wave is traveling into denser medium. Figure 10 shows the stress at the wave front as a function of time for the cases of constant density and varying density.

The integration of the differential eq. (52) needs a knowledge of d^2q/dT^2 at $T=0$. This has been obtained by differentiating the equation of conservation of momentum along the wave front and using the limiting process as k tends to zero.

XIII. Two Stage Locking

The constitutive relationship for a two stage locking material is shown in Fig. 11. These relationships can be written in the form of equations
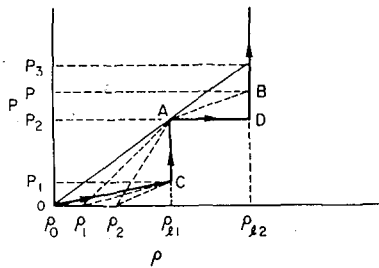

Fig. 11.

For $P \leq P_1$ $\qquad\qquad$ $P = P_1(\rho/\rho_0 - 1)/(\rho_{l1}/\rho_0 - 1)$. $\qquad\qquad$ (54)

For $P_1 \leq P \leq P_2$ $\qquad\qquad$ $\rho = \rho_{l1}$. $\qquad\qquad$ (55)

For $P \geq P_2$ $\qquad\qquad$ $\rho = \rho_{l2}$. $\qquad\qquad$ (56)

As before, the material is assumed to have no shear resistance, $i.\,e.$,

$$\sigma_x - \sigma y = 0. \qquad\qquad (57)$$

Then $P-\rho$ curve represents the $\sigma_x - \rho$ diagram. Because very little is known about unloading characteristics, only the case of loading will be considered.

The problem of sudden application of pressure $P > P_2$ at the surface $x = a(t)$ will be discussed. The wave pattern will be different depending on whether P is greater than P_3 or less than P_3 (Fig. 9). If $P > P_3$, there is one shock wave and the density behind the shock wave is equal to ρ_{l2}. However, for pressures less than the value of P_3 there is a two shock wave structure. The explanation for such behavior can be found in the paper of Duvall (1962 c) where a complete study of shock stability in solids has been presented.

XIV. Case of $P < P_3$

In the one-dimensional system under uniaxial strain conditions the initial density distribution has been assumed to be given by eqs. (26) and (27). For a pressure $P_2 < P < P_3$ two shock waves will be propagating in the material. Let the position be denoted by

* In these cases $\bar{P}(t) = \bar{P}(0)$.

$x=k_{12}(t)$ and $x=k_{23}(t)$. The wave velocities are proportional to the square root of the slope of the secants OA and AB. Initially the slope of OA corresponds to that of the line joining $(P=0, \rho=\bar{\rho}_0)$ to the point $(P=P_2, \rho=\rho_{l1})$. The slope of the line is definitely greater than that of AB. Therefore the shock wave changing the pressure from zero to P_2 will travel faster than the shock wave across which the pressure changes from P_2 to P. Then the region in an x–t plane can be separated into the following regions (Fig. 12).
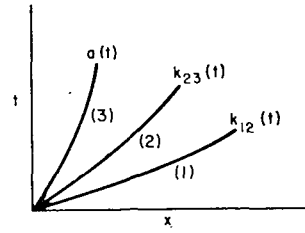
Fig. 12.

1. $x>k_{12}(t)$, which is undisturbed.
2. $k_{23}(t)<x<k_{12}(t)$. In this region the pressure changes from zero to P_2.
3. $a(t)<x<k_{23}(t)$. In this region the pressure changes from P_2 to P.

In the region 1

$$u_1 = 0, \tag{58}$$

$$\sigma_{x1} = 0. \tag{59}$$

The subscript (1) in these equations denotes the region in which the solutions are valid. In region 2 the material locks at the locking density ρ_{l1}. The general solution in this region can be written following eqs. (17) and (18).

$$u_2 = f_2(t), \tag{60}$$

$$\sigma_{x2} = \rho_{l1} x \dot{f}_2(t) + g_2(t). \tag{61}$$

Similarly, the stresses and velocities in region 3 are

$$u_3 = f_3(t), \tag{62}$$

$$\sigma_{x3} = \rho_{l2} x \dot{f}_3(t) + g_3(t). \tag{63}$$

The unknown functions f_2, f_3, g_2, g_3, as well as the position of the wave fronts $k_{12}(t)$, $k_{23}(t)$, and the position of the inner surface $a(t)$ can be determined from boundary and initial conditions in the following way.

Boundary and initial conditions. The stress jumps from P_2 to a higher value across the wave front $x=k_{23}(t)$. This result can also be deduced from thermodynamic considerations and shock stability. Then at

$$x = k_{23}(t), \qquad \sigma_{x2} = -P_2. \tag{64}$$

From eqs. (61) and (64)

$$g_2(t) = -P_2 - \rho_{l1} k_{23} \dot{f}_2(t), \tag{65}$$

and

$$\sigma_{x2} = \rho_{l1}(x-k_{23}) \dot{f}_2(t) - P_2. \tag{66}$$

The jump conditions at $x=k_{12}$ are

$$\rho_0 \dot{k}_{12} = \rho_{l1}(\dot{k}_{12}-u_2), \tag{67}$$

$$\rho_{l1}(\dot{k}_{12}-u_2) u_2 = -\sigma_{x2}. \tag{68}$$

Then

$$f_2(t) = u_2 = \dot{k}_{12}\left[1 - \frac{\rho_0(k)}{\rho_{l1}}\right], \tag{69}$$

and

$$\rho_{l1}\left\{\dot{k}_{12}-\dot{k}_{12}\left[1-\frac{\rho_0(k)}{\rho_{l1}}\right]\right\}\ \left[1-\frac{\rho_0(k)}{\rho_{l1}}\right]\dot{k}_{12} = -\rho_{l1}(k_{12}-k_{23})\,\dot{f}_2(t)+P_2\,. \tag{70}$$

For

$$\rho_0(k) = \bar{\rho}_0\,, \tag{71}$$

where $\bar{\rho}_0$ is a constant, eq. (70) then reduces to

$$\rho_{l1}\beta_1(1-\dot{\beta}_1)\,\dot{k}_{12}^2+\rho_{l1}(k_{12}-k_{23})\,\ddot{k}_2\beta_1-P_2 = 0\,, \tag{72}$$

where

$$\beta_1 = 1-\frac{\bar{\rho}_0}{\rho_{l1}}\,. \tag{73}$$

The pressure at the left boundary is assumed to be prescribed.

$$x = a(t) \qquad \sigma x_3 = -\bar{P}(t)\,.$$

Then

$$g_3(t) = -P-\rho_{l2}a\dot{f}_2(t)\,, \tag{74}$$

and

$$\sigma_{x3} = \rho_{l2}(x-a)\,\dot{f}_3(t)-P(t)\,. \tag{75}$$

The jump conditions at $x=k_{23}(t)$ are

$$\rho_{l2}(\dot{k}_{23}-u_3) = \rho_{l1}(\dot{k}_{23}-u_2)\,, \tag{76}$$

and

$$\rho_{l2}(\dot{k}_{23}-u_3)\,u_3-\rho_{l1}(\dot{k}_{23}-u_2)\,u_2 = -\sigma_{x3}+\sigma_{x2}\,. \tag{77}$$

Equation (76) can be simplified to the following form

$$u_3 = \dot{k}_{23}\left(1-\frac{\rho_{l1}}{\rho_{l2}}\right)+\frac{\rho_{l1}}{\rho_{l2}}u_2\,. \tag{78}$$

Then

$$f_3(t) = \beta_2\dot{k}_{23}+\frac{\rho_{l1}}{\rho_{l2}}f_2(t)\,, \tag{79}$$

where

$$\beta_2 = 1-\frac{\rho_{l1}}{\rho_{l2}}\,. \tag{80}$$

By substituting eqs. (66), (69), (75) and (79) in eq. (77), the following equation can be obtained.

$$\rho_{l2}\left(\dot{k}_{23}-\beta_2\dot{k}_{23}-\frac{\rho_{l1}}{\rho_{l2}}\beta_1\dot{k}_{12}\right)\left(\beta_2\dot{k}_{23}+\frac{\rho_{l1}}{\rho_{l2}}\beta_1\dot{k}_{12}\right)-\rho_{l1}(\dot{k}_{23}-\beta_1\dot{k}_{12})\beta_1\dot{k}_{12}$$

$$= -\rho_{l2}(k_{23}-a)\left[\beta_2\ddot{k}_{23}(t)+\frac{\rho_{l1}}{\rho_{l2}}\beta_1\ddot{k}_{12}\right]+P(t)-P_2\,. \tag{81}$$

$a(t)$ in eq. (81) can be eliminated by considering the conservation of mass of the region $x<k_{12}(t)$.
Then

$$\rho_0 k_{12} = \rho_{l1}(k_{12}-k_{23})+\rho_{l2}(k_{23}-a)\,. \tag{82}$$

Equation (81) now becomes

$$\rho_{l2}\left(\dot{k}_{23}-\beta_2\dot{k}_{23}-\frac{\rho_{l1}}{\rho_{l2}}\beta_1\dot{k}_{12}\right)\left(\beta_2\dot{k}_{23}+\frac{\rho_{l1}}{\rho_{l2}}\beta_1\dot{k}_{12}\right)-\rho_{l1}(\dot{k}_{23}-\beta_1\dot{k}_{12})\beta_1\dot{k}_{12}$$

$$=-\rho_{l2}\left[\rho_0 k_{12}-\rho_{l1}(k_{12}-k_{23})\right]\left[\beta_2\ddot{k}_{23}+\frac{\rho_{l1}}{\rho_{l2}}\beta_1\ddot{k}_{12}\right]+P(t)-P_2\,. \tag{83}$$

Equations (72) and (83) are two equations for two unknowns $k_{12}(t)$ and $k_{23}(t)$. If these equations are integrated subject to appropriate initial conditions, the position of the wave front, stress and velocities can be obtained. The results are shown in Figs.
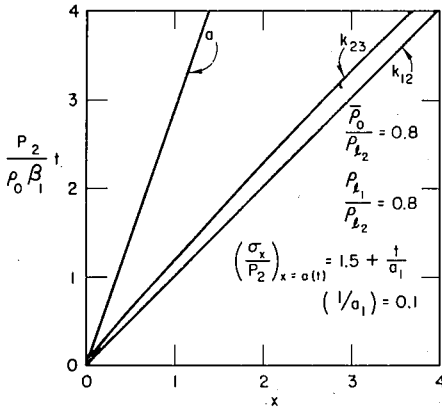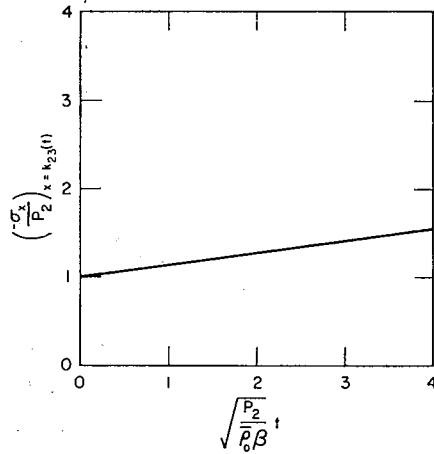

Fig. 13.

Fig. 14.

13 and 14. Figure 13 shows the position of wave fronts. Figure 14 illustrates the stress distribution at the wave front k_{23}.

The initial conditions are

$$t=0\,,\qquad k_{12}=k_{23}=0\,,$$

$$\dot{k}_{12}=\sqrt{\frac{P_2}{\rho_0\beta_1}}\,,\qquad \dot{k}_{23}=\beta_1\dot{k}_{12}\sqrt{\frac{P_{(0)}-P_2}{\rho_{l1}\beta_2}}\,.$$

The integrations have been carried out for the case in which $P(t)$ increases linearly with time.

XV. Dynamic Constitutive Relations and Phase Changes

So far the discussions are based on the assumption that the static stress-strain relationships are valid in dynamic problems. Also, the components of stress tensor other than the hydrostatic pressure has been neglected.

It is very well known that static conditions can be attained in a dynamic problem as time tends to infinity. The constitutive relations in a dynamic problem could be quite different from that observed in static experiments. The only conditions are that these relations should govern the static results at large times. Similarly, the dynamic phase changes could follow a process very different from the static process of phase changes.

In this section dynamic effects on the constitutive relations and the effect of the complete stress tensor will be considered. The assumptions of uniaxial strain, however.

will be retained. Thermodynamic effects will not be considered.

The stress tensor σ_{ij} can be separated into hydrostatic pressure p and the extra stress tensor σ'_{ij}

$$\sigma_{ij} = -p\delta_{ij}+\sigma'_{ij}, \tag{84}$$

under the assumption of uniaxial strain the x direction

$$p = 1/3\,(\sigma_x+2\sigma_y), \tag{85}$$

$$\sigma'_{11} = 2/3\,(\sigma_x-\sigma_y), \tag{86}$$

$$\sigma'_{22} = \sigma'_{33} = 1/3\,(\sigma_y-\sigma_x), \tag{87}$$

$$\sigma'_{12} = \sigma'_{23} = \sigma'_{13} = 0. \tag{88}$$

If the stress-strain relationships observed in static experiments were valid for the dynamic problem, the pressure p can be assumed to be a function of density and $(\sigma_x-\sigma_y)$ can be assumed to vary according to the elastic-ideal plastic behavior. The yield conditions can be of Tresca, Misses or Coloumb type.

The dynamic constitutive relations will be illustrated by a simple variation from the static type of stress-strain relationship.

If

$$|\sigma_x-\sigma_y|<y, \tag{89}$$

$$\sigma_x-\sigma_y = 2G\,(\dot{\varepsilon}_x), \tag{90}$$

where y is the static yield stress. If

$$|\sigma_x-\sigma_y|>y,$$

a constitutive relationship of the following form can be assumed.

$$\hat{\sigma}'_{ij}{}^{\dagger} = F(\sigma). \tag{91}$$

In this equation $\hat{\sigma}'_{ij}$ is the first stress rate, $\dot{\varepsilon}_j$ is the rate of strain tensor and ρ is the density. In the case of uniaxial strain the rate of strain tensor can be written as

$$\dot{\varepsilon}_{ij} = \dot{e}\delta_{ij}+\dot{\varepsilon}'_{ij}, \tag{92}$$

where

$$\dot{e} = 1/3\,(\dot{\varepsilon}_x+2\,\dot{\varepsilon}_y), \tag{93}$$

$$\dot{\varepsilon}'_{11} = 2/3\,(\dot{\varepsilon}_y-\dot{\varepsilon}_x), \tag{94}$$

$$\dot{\varepsilon}'_{22} = \dot{\varepsilon}'_{33} = 1/3\,(\dot{\varepsilon}_y-\dot{\varepsilon}_x), \tag{95}$$

$$\dot{\varepsilon}'_{12} = \dot{\varepsilon}'_{23} = \dot{\varepsilon}'_{31} = 0. \tag{96}$$

Then a simple relationship of the form eq. (91) is

$$\hat{\sigma}'_{11} = F(\sigma'_{11}, \dot{\varepsilon}'_{11}, \rho). \tag{97}$$

This equation can be generalized to include higher stress rates and strain rates. A specific form of eq. (97) can be written as

$$\dot{\varepsilon}'_{11} = \frac{\sigma'_{11}-\theta y}{2GT} + \frac{\dot{\varepsilon}'_{11}}{2G}, \tag{98}$$

---

† $\frown$ indicates the Jaumann or Corotational stress rates (Noll and Truesdell, 1964).

and

$$\theta = \pm 1 . \tag{99}$$

This equation indicates that stress deviator can exceed the value of the static yield stress y. However, these stresses relax towards the yield stress with time. The constant θ takes care of the fact that yielding can take place when the stress deviator exceeds a positive or negative maximum. G in eq. (97) is the modulus of rigidity and T is a constant having the dimension of time.

In order to study simple variations from the usual static stress-strain relationships the assumption of p as a function of density and the locking characteristics will be retained. Only single stage locking will be considered. Equations (14), (15) and the constitutive relations define the problem. The hyperbolicity of the equations can be shown by determining the real characteristics.

$$u, u \pm \sqrt{\frac{\partial p}{\partial \rho} + \frac{4G}{3\rho}} .$$

Integration of these equations subject to the appropriate boundary and jump conditions will not be discussed here. Some results are shown Fig. 15.
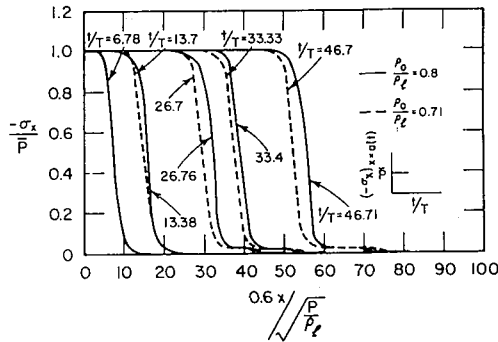

Fig. 15.

It is assumed that a constant pressure $\bar{P}$ is applied at the left boundary $x = a(t)$. The resulting variation of δ_x with x at various intervals of time are shown in Fig. 15. In this case $p - \rho$ relationship is according to single stage locking behavior. The stress deviator strain rates are related according to eq. (98). It can be seen that the stress jump initially travels as a single shock wave as though the material were elastic. However as time increases the stress deviator or the shear stresses relax towards the yield stress and the elastic precessor wave is formed which travels faster than the shock wave.

The profile of stress versus x at large times would be the one that can be seen at $t/T = 33$. This would be the stress-time profile that would be obtained by calculations using static stress-strain relationship.

These figures show the different dynamic behavior at early times after loading. These transient behavior, however, reduce to the usual steady state case after sometime.

In order to obtain more quantitative results, more general constitutive relationships, thermodynamic effects and experimental work is necessary. This paper has discussed only certain aspects of foundation to the study of snow at high pressures.

References

1) Anderson, D. L. and Benson, C. S. 1963 The densification and diagenesis of snow. In Ice and Snow (W. D. Kingery, ed.), M. I. T. Press, Cambridge, Mass., 391–411.

2) Bridgeman, P. W. 1911 Water in liquid and five solid forms under pressure. Proc. Amer. Acad. Arts Sci., 47, 441–558.

3) Bridgeman, P. W. 1912 Thermodynamic properties of liquid water to 80° and 12,000 kgm. Proc. Amer. Acad. Arts Sci., 48, 309–362.

4) Bridgeman, P. W. 1914 High pressures and five kinds of ice. J. Franklin Inst., 177, 315–332.

5) Bridgeman, P. W. 1937 The phase diagram of water to 4500 kg/cm². J. Chem. Phys., 5, 964–966.

6) Bridgeman, P. W. 1941 Freezings and compressions to 50,000 kg/cm². J. Chem. Phys., 9, 794–797.

7) Costes, N. C. 1963 On the process of normal snow densification in an ice cap. In Ice and Snow (W. D. Kingery, ed.), M. I. T. Press, Cambridge, Mass., 412–431.

8) Doran, D. G. and Linde, R. K. 1966 Shock effects in solids. (To be published).

9) Duvall, G. E. 1962 a Shock wave in the study of solids. Appl. Mech. Rev., 15, 849–854.

10) Duvall, G. E. 1962 b Concepts of shock wave propagation. Bull. Seis. Soc. Amer., 52, 869–893.

11) Duvall, G. E. 1962 c Shock wave stability in solids. In Les Ondes de Detonation, Centre National de la Recherche Scientifique, Paris, 337–352.

12) Duvall, G. E. 1963 Propagation of plane shock waves in a stress-relaxing medium. Proc. Intern. Symposium on stress waves in anelastic solids (preprint), Brown Univ.

13) Flugge, W. and Hanagud, S. 1963 A contribution to the theory of isotropic locking. SUDAER 152, Dept. of Aeronautics and Astronautics, Stanford Univ., 162 pp.

14) Grigorian, S. S. 1956 Basic concepts of soil dynamics. Priklad. Mat. i Mekh. (USSR), 24, 1057–1083.

15) Hanagud, S. 1966 Finite amplitude waves in a locking-relaxing solid. In Research Lecture, Proc. Vth U. S. National Congress on Applied Mechanics, 63–77.

16) Mellor, M. 1962 Polar snow—A summary of engineering properties. In Ice and Snow (W. D. Kingery, ed.), M. I. T. Press, Cambridge, Mass., 528–559.

17) Noll, W. and Truesdell, C. 1964 The nonlinear field theory of mechanics. In Encyclopedia of physics (S. Flugge, ed.), preprint.

18) Prager, W. 1956 a Elastic solids of limited compressibility. C 11–16, Tech. Rept., 16, Div. of Appl. Math, Brown Univ.

19) Prager, W. 1956 b On limiting states of deformation, C 11–16, Tech. Rept., 9, Div. of Appl. Math, Brown Univ.

20) Rice, M. H., McQueen, R. C. and Walsh, J. M. 1958 Compression of solids by strong shock waves. In Solid State Physics, 6 (F. Seitz and D. Turnbull, eds.), 1–63.

21) Wuori, A. F. 1963 Snow stabilization studies. In Ice and Snow (W. D. Kingery, ed.), M. I. T. Press, Cambridge, Mass., 438–458.

22) Yosida, Z. 1962 Physical properties of snow. In Ice and Snow (W. D. Kingery, ed.), M. I. T. Press, Cambridge, Mass., 485–527.